Halogen Bonding

International Edition: DOI: 10.1002/anie.201507229
German Edition: DOI: 10.1002/ange.201507229

# Halogen Bonding to Amplify Luminescence: A Case Study Using a Platinum Cyclometalated Complex

*Vasily V. Sivchik, Anastasia I. Solomatina, Yi-Ting Chen, Antti J. Karttunen, Sergey P. Tunik, Pi-Tai Chou,* and Igor O. Koshevoy**

***Abstract:*** *The cocrystallization of a weakly luminescent platinum complex [Pt(btpy)(PPh$_3$)Cl] (**1**) (Hbtpy = 2-(2-benzothienyl)pyridine; emission quantum yield $\Phi_{em} = 0.03$) with fluorinated bromo- and iodoarenes $C_6F_{6-n}X_n$ (X = Br, I; n = 1, 2) results in the formation of efficient halogen-bonding (XB) interactions Pt−Cl···X−R. An up to 22-fold enhancement ($\Phi_{em} = 0.65$) in the luminescence intensity of the cocrystallized compound is detected, without a substantial change of the emission energy. Based on crystallographic, photophysical, and theoretical investigations, the contribution of the XB donors $C_6F_{6-n}X_n$ to the amplification of luminescence intensity is attributed to the enhancement of spin–orbit coupling through the heavy-atom effect, and simultaneously to the suppression of the nonradiative relaxation pathways by increasing the rigidity of the chromophore center.*

Noncovalent attractive interactions, such as hydrogen, halogen, or metallophilic bonding as well as π–π stacking, are widely used for the design and fabrication of a variety of functional materials, constructed from organic, inorganic, or organometallic building blocks. These diverse assemblies of different levels of complexity are capable of certain unique actions, such as a detectable response to an external physical or chemical stimulus, energy transfer, or energy conversion.[1] In yet another approach, halogen bonding (XB)[2] has been recognized as an effective tool in crystal engineering.[3] A deeper understanding of XB-driven aggregation in the solid state led to a number of supramolecular systems with attractive physical characteristics, which include modified surfaces,[4] organic gels,[5] charge-transfer electroactive species,[6] liquid crystals,[7] and optically active compounds.[8] Despite the considerable progress which has been achieved in the construction of XB-stabilized architectures, the exploration of the XB phenomenon for the development of light-generating materials remains in its infancy. The vast majority of reports on this topic deal with the activation of phosphorescence from purely organic compounds by cocrystallization with a suitable haloaromatic partner.[8] Cocrystallization induces XB formation, leading to an enhanced external-heavy-atom effect facilitating spin–orbit coupling and consequently intersystem crossing, resulting in efficient triplet emission.

In contrast, very few studies on the effect of XB on the optical properties of transition-metal complexes, a large class of luminophores, have been reported to date. Halogen bonds were used to construct supramolecular assemblies containing weakly luminescent cyanometallates $[Ru(diimine)(CN)_4]^{2-}$, however the assemblies displayed no improvement of emission intensity.[9] Recently, luminescence quenching of a rotaxane incorporating the [Re(diimine)(CO)$_3$] chromophore was explained by strong binding of $I^-$ in solution.[10] Herein, we describe the first example of the dramatic enhancement of luminescence intensity of a metal complex in the solid state upon cocrystallization with XB donors.

The concept of XB implies an attractive interaction between an X′−R moiety ( that is, an XB donor acting as Lewis acid; X′ is a polarizable electrophilic halogen, R is an electron-withdrawing organic group), and an appropriate nucleophilic atom Y (the Lewis base/XB acceptor; Y = N, O, S, Se, or halogens).[3a] The inorganic or organometallic compounds M−Y serve as acceptor moieties to give the general structure M−Y···X′−R, where Y is conventionally an anionic $CN^-$, $SCN^-$, oxide, or halide ligand.[11]

Platinum(II) halide cyclometalated species are known to be versatile luminophores,[12] prompting us to investigate if it might be possible to modulate their photophysical properties utilizing halogen bonding. Accordingly, complex [Pt(btpy)(PPh$_3$)Cl] (**1**) (Hbtpy = 2-(2-benzothienyl)pyridine) was synthesized in high yield following a general cyclometalation method (Scheme 1).[13]

The benzothienyl pyridine ligand was primarily chosen because of the electron richness of the thiophene moiety, which is expected to increase the nucleophilicity of the *trans* chloride in the resulting compound and thus facilitate its participation as a Lewis base in XB formation. The single-crystal XRD analysis of deep-yellow crystals of **1**[14] reveals that the complex has a geometry typical of [Pt(C^N)(PR$_3$)X] compounds (C^N = carbometalated imine ligand), with a chloride located *trans* to the deprotonated C atom (Figure 1, left).[15] The structural parameters for the crystal structure of **1** are also not exceptional (see the Supporting Information, Table S2).[15] Though no metal–metal contacts

[*] V. V. Sivchik, Prof. I. O. Koshevoy
Department of Chemistry, University of Eastern Finland
80101 Joensuu (Finland)
E-mail: igor.koshevoy@uef.fi
A. I. Solomatina, Prof. S. P. Tunik
Department of Chemistry, St. Petersburg State University
Universitetskii pr. 26, 198504 St. Petersburg (Russia)
Y.-T. Chen, Prof. P.-T. Chou
Department of Chemistry, National Taiwan University
Taipei 106 (Taiwan)
E-mail: chop@ntu.edu.tw
Prof. A. J. Karttunen
Department of Chemistry, Aalto University
00076 Aalto (Finland)

Supporting information for this article is available on the WWW under http://dx.doi.org/10.1002/anie.201507229.

  

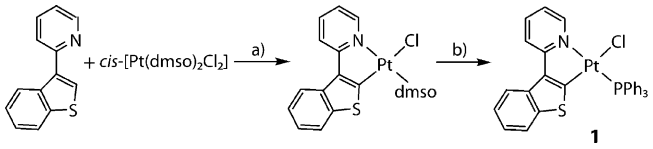


***Scheme 1.*** Synthesis of complex **1**: a) $NaOOCCH_3$, methanol/toluene 1:20 (v/v), 90 °C, 40 h, 94 %; b) $PPh_3$, $CH_2Cl_2$, 2 h, 25 °C, 90 %. dmso = dimethylsulfoxide.

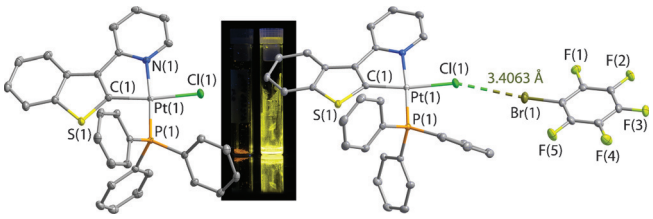


***Figure 1.*** Molecular views of complexes **1** (left) and **2a** (right). Thermal ellipsoids are set at 50 % probability. Inset: emission of the compounds under UV light irradiation ($\lambda = 365$ nm).

were found, the crystal structure shows some π–π stacking because of the partial overlap between the btpy π systems of two adjacent molecules organized in a head-to-tail manner with an interplanar distance of circa 3.35 Å (Figure S1). Complex **1** is not luminescent in solution at 298 K and in the solid state exhibits rather weak emission with quantum yield ($\Phi_{em}$) of 0.03 at room temperature (Figure 2; see Table 1). The emission spectral profile of **1** is structured, exhibiting a vibronic progression of circa 1350–1500 $cm^{-1}$ typical of aromatic chromophores. When taken together, the spectral profile of **1**, the absence of Pt···Pt interactions, and the excited-state lifetime in the microsecond domain ($\tau_{obs} =$ 2.2 μs; Table 1) indicate that the excited state responsible for the luminescence is of triplet origin (phosphorescence), with the most dominant contribution from btpy ligand-centered ($^3\pi\pi$) transitions possibly mixed with some metal-to-ligand charge transfer (MLCT). The computational studies of the lowest-energy excited state (DFT-PBE0/def2-TZVP level of theory; Figure S5) support this assignment.

Interestingly, grinding complex **1** with an excess of bromopentafluorobenzene (Br-F5 b) results in the immediate lightening of the sample color from deep to pale yellow with the formation of complex **2a**. The emission intensity from **1** to **2a** also increases significantly (Figure 1, inset; Table 1). The X-ray structure of **2a** (Figure 1, right)[14] shows the presence of a short Cl···Br contact (3.4063(7) Å) that corresponds to an $R_{XX'}$ value of 0.946 ($R_{XX'} = d(X\cdots X')/(r_X + r_{X'})$, where $d$ is the distance and $r_X$ and $r_{X'}$ are the van der Waals (vdW) radii of the halogens).[16] The Cl···Br distance measures 5.4 % less than the sum of the vdW radii (3.60 Å) pointing to a relatively weak XB. The bond angles in **2a** (Pt-Cl···Br and Cl···Br-C angles are 161.72 and 160.89°, respectively) indicate a type I halogen–halogen contact[17] that has nearly equal M-X···X′ and X···X′-R angles in the range 150–160° for metal halides.[16] Though type I contacts are thought to be predominantly electrostatic in nature to minimize repulsion between the halogens, the Pt–Cl bond in **2a** (2.3566(6) Å) is slightly longer than that in **1** (2.3470(4) Å), which suggests an attractive-like interaction. The crystal packing of **2a** (Figure S2) is supported by π–π interactions.

Using iodopentafluorobenzene (I-F5 b) instead of Br-F5 b afforded complex **2b**, which is isomorphous to **2a** showing only minor variations in the unit-cell dimensions (Figure S2 and Table S1).[14] The M–X···X′–R contacts become stronger with an increase in the atomic number of the X′ moiety.[16] Indeed, the Cl···I distance in **2b** (3.3330(5) Å) is shorter than the analogous Cl···Br value in **2a** and is 10.6 % shorter than the sum of the corresponding vdW radii (3.73 Å; $R_{XX'} =$ 0.894). The shortness of the bond length is unprecedented for type I halogen contacts and is within the range of strong M–X···X′–R bonds.[16] The Pt–Cl bond in **2b** (2.3627(4) Å) is longer than that measured for **1**. Computational analysis of the structures of **2a** and **2b** also points to the attractive character of the type I bonding, which results in bond energies of −9(−12) and −15(−22) kJ $mol^{-1}$ for Cl···Br and Cl···I contacts, respectively, for experimental and optimized (given in parentheses) geometries (Table S3).

To extend the series, we employed bifunctional XB donors 1,4-dibromo- and 1,4-diiodotetrafluorobenzenes (2 Br-F4 b and 2 I-F4 b) to obtain the dimeric assemblies {[Pt(btpy)-$(PPh_3)$Cl]}$_2$·2 Hal-F4 b (**3a**: Hal = Br; **3b**: Hal = I). As evident for their mononuclear congeners, **3a** and **3b** form isomorphous crystals. Their structures (Figure 3 and Figure S3)[14] reveal that molecules 2 Br-F4 b and 2 I-F4 b each symmetrically link two Pt fragments. The geometry of the halogen–halogen interaction is significantly different from that detected for **2a/b** and can be classified as a type II contact.[18]

The Cl···Hal-C angles are close to linear (173.34 and 173.24° for **3a** and **3b**, respectively), while the Pt-Cl···Hal angles are noticeably bent (109.10 and 104.60°). This pronounced directionality is the optimum arrangement for XB and allows for effective contact between the nucleophilic region of the XB donor (iodine) and the electrophilic region of the XB acceptor (chloride).[18] The Cl···Hal distances in **3a/b** (3.2354(5)/3.2001(3) Å) are markedly shorter than in **2a/b**, which can be accounted for stronger halogen interactions. The Cl···Hal contacts in **3a/b** are 10.1 % ($R_{XX'} = 0.899$) and 14.2 % ($R_{XX'} = 0.858$) shorter than those in the previously reported [Pd(PCP)Cl·2 I-F4 b] system.[11c] According to the theoretical results, net XB energies in the dinuclear species **3a/b** for the

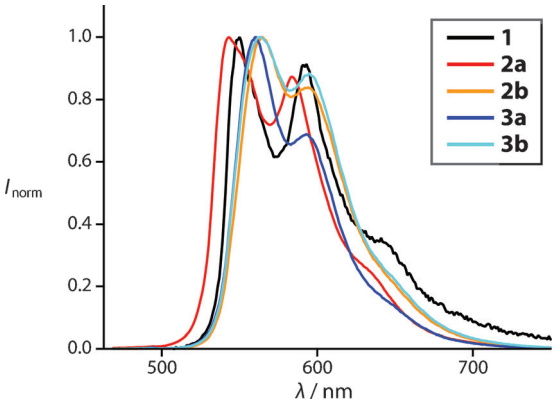


***Figure 2.*** Normalized solid-state emission spectra of **1**–**3** at 298 K. Excitation wavelength $\lambda_{exc} = 400$ nm.

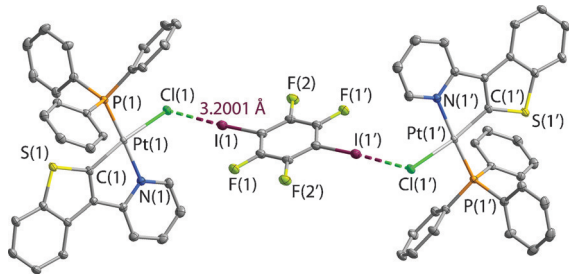


***Figure 3.*** Molecular view of complex **3b**. Thermal ellipsoids are set at 50% probability.

experimental (and optimized) geometries are −25(−29) and −43(−46) kJ mol$^{-1}$, respectively, giving −12.5(14.5) and −21.5(23) kJ mol$^{-1}$ per Cl···Hal contact (Table S3). Although these estimations of energies may not be absolutely precise, they adequately describe a general trend detected for compounds **2a/b** and **3a/b** and therefore indicate that there might be a rather minor energetic difference between halogen contacts of types I and II under certain conditions. Similar to **2a/b**, some π–π interactions are seen in **3a/b** (Figure S4), which, together with appreciable intermolecular F···H contacts, stabilize the crystal packing.

To gain more insight into the XB-associated properties, we then investigated the photophysical characteristics of these complexes. In solution, the compounds are virtually non-luminescent, which led us to focus on their emissive properties in the crystalline solid state. Pertinent photophysical parameters of crystalline compounds **1**–**3** (at 298 K) are listed in Table 1.

In comparison to the weak emission intensity of **1** ($\Phi_{em}$ = 0.03), cocrystallization of **1** with XB donors Br-F5b and I-F5b to form compounds **2a** and **2b** results in a remarkable 10- and 22-fold increase of the emission quantum yield. The highest value is reported for compound **2b**, which has an emission quantum yield $\Phi_{em} = 0.65$. In addition to the changes in $\Phi_{em}$ values, the observed emission excited-state lifetimes ($\tau_{obs}$) increase significantly from 2.2 μs in **1** to 14.8 μs and 24.3 μs in **2a** and **2b**, respectively. The emission intensity of binuclear compounds **3a/b** are also significantly enhanced ($\Phi_{em} = 0.21$ and 0.31 for **3a** and **3b**, respectively) when compared with **1**, but are slightly lower than those of related compounds **2a/b**. The observed lifetimes for **3a/b** (9.5 and 7.5 μs) follow the same trend as the $\Phi_{em}$ values and are significantly longer than those measured for compound **1**. The radiative decay rate constants ($k_r$) can be deduced from the values of emission lifetime and quantum yield and the corresponding parameters are listed in Table 1. The $k_r$ values for all compounds are found to be less than $10^5$ s$^{-1}$, affirming that the emission from these complexes is phosphorescence. Additionally, for complexes **2a/b** and **3a/b**, the radiative lifetimes on the μs timescale and the vibronic progression (similar to that of **1**) evident in the emission spectra would suggest that the origin of the emission is the same as that for **1**, largely attributable to a btpy ligand-centered $^3\pi\pi^*$ excited state for **2a/b** and **3a/b**. The results of the computational analysis also show that the lowest-energy excited is practically identical for all complexes (Supporting information). In other words, despite the drastic increase of the emission intensity, the XB donors only have a slight influence on the nature of the frontier orbitals participating in emissive electronic transitions (Figure S5) and their contribution is largely to suppress nonradiative excited-state relaxation pathways (see the $k_{nr}$ values in Table 1).

***Table 1:*** Photophysical properties of complexes **1**–**3** in the solid state at 298 K.

| Complex | $\lambda_{em}$ [nm] | $\tau_{obs}$ [μs] | $\Phi_{em}$ | $k_r$ [s$^{-1}$][a] | $k_{nr}$ [s$^{-1}$][b] |
|---|---|---|---|---|---|
| **1** | 560, 594 | 2.2 | 0.03 | $1.4\times10^4$ | $4.4\times10^5$ |
| **2a** | 543, 585 | 14.8 | 0.32 | $2.2\times10^4$ | $4.5\times10^4$ |
| **2b** | 565, 595 | 24.3 | 0.65 | $2.7\times10^4$ | $1.4\times10^4$ |
| **3a** | 560, 593 | 9.5 | 0.21 | $2.2\times10^4$ | $8.3\times10^4$ |
| **3b** | 563, 595 | 7.5 | 0.31 | $4.1\times10^4$ | $9.2\times10^4$ |

[a] $k_r = k_{obs} \times \Phi_{em}$ where $k_{obs} = 1/\tau_{obs}$;. [b] $k_{nr} = k_{obs} - k_r$.

The significant XB-induced emission enhancement is remarkable and may be rationalized by the combination of two factors: a) the increase of the radiative decay rate constant $k_r$ upon formation of the halogen bond and b) the reduction of nonradiative deactivation pathways. Clearly, the XB interaction in **2a/b** and **3a/b** leads to an approximate two- to threefold increase of the $k_r$ value compared to **1** (Table 1). Moreover, the Pt–Cl···I contact is shorter (and therefore stronger) than the Pt–Cl···Br distance. Therefore, the increasing contribution of the halogen interaction from Br to I is in accordance with the greater spin–orbit coupling constant from Br to the heavier I atom, yielding greater singlet–triplet ($S_1$–$T_1$) mixing and hence an enhanced $T_1 \rightarrow S_0$ transition dipole moment, that is, an increase of the phosphorescence radiative decay rate constant.

On the other hand, circa 10- and 30-fold decreases in the nonradiative decay rate constant ($k_{nr}$) are measured for complexes **2a** and **2b** compared to that of **1**, with the stronger Cl···Hal interaction giving the lower $k_{nr}$ value. This result suggests that the nature of the bonding in the studied systems is complex and that the subtle effects of XB and crystal packing synergistically influence the relaxation of the platinum luminophore. We thus tentatively attribute the significant decrease in the radiationless deactivation of **2a/b** to a significant increase in the rigidity of the complex. This effect arises from the XB-induced weak intermolecular π stacking between btpy π systems and Br-F5b (or I-F5b) and in part the F···H contacts (Figure S2), which impede the rotational/vibrational motion of the luminophore moiety, greatly suppressing the nonradiative decay pathways. A similar trend of decreasing $k_{nr}$ values compared to **1** is measured for **3a/b**, although the decrease is not as significant as that measured for complexes **2a/b** (Table 1). This may be due to the lack of btpy/2Br-F4b (2I-F4b) π-stacking interactions in **3a/b** (Figure S4) despite the existence of two halogen bonds per XB donor. The measured photophysical parameters are indicative of the intrinsic differences between type I and type II halogen bonds in terms of geometry, leading to the observed diversity in the constructed molecular frameworks.

In summary, cocrystallization of various XB donors with platinum complex **1** leads to the formation of species which have increased radiative decay rates as a result of enhanced

  

spin–orbit coupling. Additionally, the enhanced structural rigidity of the complexes suppresses nonradiative decay rates. As a result of both factors, the cocrystallized compounds exhibit a 7- to 22-fold increase in phosphorescence intensity compared to parent complex **1**. The formation of XB occurs without a substantial change in the electron-density distribution, meaning a negligible change of the emission energy of the parent chromophore. The results demonstrate for the first time that halogen bonding can be used to amplify the luminescence of transition-metal complexes. Additionally, important insights into the structure, photophysics, and subtle differences between types I and II XB compounds incorporating metal complexes are presented. This work opens a new chapter in the chemistry of halogen-bonding-supported materials and crystal engineering.

## Acknowledgements

This work was financially supported by the University of Eastern Finland (strategic funding: Russian–Finnish and Spearhead projects), the Academy of Finland (grant 268993; I.O.K.), the Alfred Kordelin Foundation (A.J.K.), St. Petersburg State University (grants 0.37.169.2014 and 12.42.1271.2014), and the Russian Foundation for Basic Research (grants 14-03-00970 and 13-03-12411). Computational resources were provided by CSC—the Finnish IT Center for Science (A.J.K.).

**Keywords:** crystal engineering · halogen bonding · luminescence · noncovalent interactions · platinum complexes

**How to cite:** *Angew. Chem. Int. Ed.* **2015**, *54*, 14057–14060
*Angew. Chem.* **2015**, *127*, 14263–14266

[1] a) O. S. Wenger, *Chem. Rev.* **2013**, *113*, 3686–3733; b) A. Priimagi, G. Cavallo, P. Metrangolo, G. Resnati, *Acc. Chem. Res.* **2013**, *46*, 2686–2695; c) S. Varughese, *J. Mater. Chem. C* **2014**, *2*, 3499–3516; d) K. M.-C. Wong, M. M.-Y. Chan, V. W.-W. Yam, *Adv. Mater.* **2014**, *26*, 5558–5568; e) Z. Qi, C. A. Schalley, *Acc. Chem. Res.* **2014**, *47*, 2222–2233; f) X.-Y. Hu, T. Xiao, C. Lin, F. Huang, L. Wang, *Acc. Chem. Res.* **2014**, *47*, 2041–2051; g) J. Ding, L. Chen, C. Xiao, L. Chen, X. Zhuang, X. Chen, *Chem. Commun.* **2014**, *50*, 11274–11290; h) C. Jobbágy, A. Deák, *Eur. J. Inorg. Chem.* **2014**, 4434–4449; i) C. Rest, R. Kandanelli, G. Fernández, *Chem. Soc. Rev.* **2015**, *44*, 2543–2572; j) S. K. Singh, A. Das, *Phys. Chem. Chem. Phys.* **2015**, *17*, 9596–9612.

[2] G. R. Desiraju, P. S. Ho, L. Kloo, A. C. Legon, R. Marquardt, P. Metrangolo, P. Politzer, G. Resnati, K. Rissanen, *Pure Appl. Chem.* **2013**, *85*, 1711–1713.

[3] a) P. Metrangolo, F. Meyer, T. Pilati, G. Resnati, G. Terraneo, *Angew. Chem. Int. Ed.* **2008**, *47*, 6114–6127; *Angew. Chem.* **2008**, *120*, 6206–6220; b) K. Rissanen, *CrystEngComm* **2008**, *10*, 1107–1113.

[4] a) M. Boterashvili, M. Lahav, S. Shankar, A. Facchetti, M. E. van der Boom, *J. Am. Chem. Soc.* **2014**, *136*, 11926–11929; b) Q.-N. Zheng, X.-H. Liu, T. Chen, H.-J. Yan, T. Cook, D. Wang, P. J. Stang, L.-J. Wan, *J. Am. Chem. Soc.* **2015**, *137*, 6128–6131.

[5] L. Meazza, J. A. Foster, K. Fucke, P. Metrangolo, G. Resnati, J. W. Steed, *Nat. Chem.* **2013**, *5*, 42–47.

[6] J. Lieffrig, O. Jeannin, A. Frackowiak, I. Olejniczak, R. Swietlik, S. Dahaoui, E. Aubert, E. Espinosa, P. Auban-Senzier, M. Fourmigue, *Chem. Eur. J.* **2013**, *19*, 14804–14813.

[7] a) C. Präsang, H. L. Nguyen, P. N. Horton, A. C. Whitwood, D. W. Bruce, *Chem. Commun.* **2008**, 6164–6166; b) A. Priimagi, M. Saccone, G. Cavallo, A. Shishido, T. Pilati, P. Metrangolo, G. Resnati, *Adv. Mater.* **2012**, *24*, OP345–OP352..

[8] a) O. Bolton, K. Lee, H.-J. Kim, K. Y. Lin, J. Kim, *Nat. Chem.* **2011**, *3*, 205–2010; b) D. Yan, D.-K. Bucar, A. Delori, B. Patel, G. O. Lloyd, W. Jones, X. Duan, *Chem. Eur. J.* **2013**, *19*, 8213–8219; c) S. d′Agostino, F. Grepioni, D. Braga, B. Ventura, *Cryst. Growth Des.* **2015**, *15*, 2039–2045; d) S. Mukherjee, P. Thilagar, *Chem. Commun.* **2015**, *51*, 10988–11003.

[9] S. Derossi, L. Brammer, C. A. Hunter, M. D. Ward, *Inorg. Chem.* **2009**, *48*, 1666–1677.

[10] B. R. Mullaney, A. L. Thompson, P. D. Beer, *Angew. Chem. Int. Ed.* **2014**, *53*, 11458–11462; *Angew. Chem.* **2014**, *126*, 11642–11646.

[11] a) R. Bertania, P. Sgarbossa, A. Venzo, F. Lelj, M. Amati, G. Resnati, T. Pilati, P. Metrangolo, G. Terraneo, *Coord. Chem. Rev.* **2010**, *254*, 677–695; b) P. Sgarbossa, R. Bertani, V. Di Noto, M. Piga, G. A. Giffin, G. Terraneo, T. Pilati, P. Metrangolo, G. Resnati, *Cryst. Growth Des.* **2012**, *12*, 297–305; c) M. T. Johnson, Z. Džolić, M. Cetina, O. F. Wendt, L. Öhrström, K. Rissanen, *Cryst. Growth Des.* **2012**, *12*, 362–368.

[12] a) S.-W. Lai, C.-M. Che, *Top. Curr. Chem.* **2004**, *241*, 27–63; b) V. W.-W. Yam, K. M.-C. Wong, *Chem. Commun.* **2011**, *47*, 11579–11592; c) V. W.-W. Yam, *Pure Appl. Chem.* **2013**, *85*, 1321–1329; d) L. Murphy, P. Brulatti, V. Fattori, M. Cocchi, J. A. G. Williams, *Chem. Commun.* **2012**, *48*, 5817–5819; e) M. R. R. Prabhath, J. Romanova, R. J. Curry, S. R. P. Silva, P. D. Jarowski, *Angew. Chem. Int. Ed.* **2015**, *54*, 7949–7953; *Angew. Chem.* **2015**, *127*, 8060–8064.

[13] A. Capapé, M. Crespo, J. Granell, M. Font-Bardia, X. Solans, *Dalton Trans.* **2007**, 2030–2039.

[14] CCDC 1416549 (**1**), 1416550 (**2a**), 1416551 (**2b**), 1416552 (**3a**), and 1416553 (**3b**) contain the supplementary crystallographic data for this paper. These data can be obtained free of charge from The Cambridge Crystallographic Data Centre via www.ccdc.cam.ac.uk/data_request/cif.

[15] a) V. Sicilia, S. Fuertes, A. Martin, A. Palacios, *Organometallics* **2013**, *32*, 4092–4102; b) A. Díez, J. Forniés, A. García, E. Lalinde, M. T. Moreno, *Inorg. Chem.* **2005**, *44*, 2443–2453.

[16] G. M. Espallargas, F. Zordan, L. A. Marín, H. Adams, K. Shankland, J. van de Streek, L. Brammer, *Chem. Eur. J.* **2009**, *15*, 7554–7568.

[17] a) V. R. Pedireddi, D. S. Reddy, B. S. Goud, D. C. Craig, A. D. Rae, G. R. Desiraju, *J. Chem. Soc. Perkin Trans. 2* **1994**, 2353–2360; b) A. Mukherjee, G. R. Desiraju, *IUCrJ* **2014**, *1*, 49–60.

[18] P. Metrangolo, G. Resnati, *IUCrJ* **2014**, *1*, 5–7.

Received: August 3, 2015
Published online: September 25, 2015

  